

QUANTITATIVE CHEMICAL ANALYSIS OF MINERALS IN THIN-SECTION WITH THE X-RAY MACROPROBE

O. DON HERMES AND PAUL C. RAGLAND, *Department of Geology, University of North Carolina at Chapel Hill.*

ABSTRACT

A curved mica crystal attachment for the standard Philips vacuum X-ray spectrograph, commercially referred to as the "macroprobe," allows the quantitative chemical analysis of small surface areas in samples of geologic interest. The instrument has been calibrated for the analysis of total Fe, Mn, Ti, Ca, and K in ferromagnesian silicate minerals. Agreement between analyses performed with the macroprobe and by other methods is generally well within 10 percent. Analyses for Fe may be made on an area about 100μ in diameter, but because of slower count rates, the other elements require a spot size of at least 460μ . The critical thickness of the thin-section to insure maximum intensity of the Fe X radiation was found to be about 70μ .

INTRODUCTION

The recent development of the electron microprobe as a quantitative analytical tool has led to opportunities for research which before were virtually impossible. The ability to perform a quantitative chemical analysis on an individual mineral or part of an inhomogeneous mineral in a rock paves the way for many fruitful studies. Unfortunately, the complex, highly specialized instrumentation and high initial cost of the microprobe means that it will be available to relatively few researchers. On the other hand, the X-ray macroprobe is relatively inexpensive and comparatively simple to operate. This paper will demonstrate that the macroprobe, although not as versatile nor as capable of fine resolution as the electron microprobe, can be used for quantitative, nondestructive chemical analysis of small surface areas in samples of geologic interest.

GENERAL DESCRIPTION

The basic component of the instrument is a curved mica crystal attachment for the standard Philips Universal vacuum X-ray spectrograph. The diameter of the X-ray beam that impinges upon the sample is confined by masking off part of the X-ray port and passing the X rays through an aperture of suitable size. The diameter of the area actually being irradiated may vary from approximately 0.1–1.0 mm., depending upon the size of the aperture. The secondary X rays emitted by elements in the sample are then diffracted and focused on the detector window by means of the curved mica crystal monochromator. For best focusing, the secondary X-ray source (*i.e.*, the sample), the crystal monochromator, and the detector window must lie on arcs of the same great circle. This is achieved by use of an X-ray optical design similar to that used in some electron

microanalyzers. It is the Ogilvie type with a varying curvature Johann focusing device (Ogilvie, 1964, 1962). The attachment is designed to permit analyses of all elements within the normal range of the X-ray vacuum spectrograph. To date the instrument has been calibrated for total Fe, Mn, Ti, Ca, and K in ferromagnesian silicate minerals.

The idea is not new; for example, Adler and Axelrod (1957) were able to semiquantitatively analyze areas down to about 0.5 mm. in diameter by masking off the primary X-ray beam and focusing the secondary X rays by means of curved crystal optics. They were able to determine the relative distribution of Fe, Co, and Se across a polished section of pyrite. The macroprobe attachment is the first commercially available unit capable of quantitative analysis which includes a light optics system for visual inspection of the sample.

The light optics system furnished with the unit can be used only for examination of opaque samples in reflected light. As shown in Figure 1, some of the light from the illuminator is reflected downward off the beam splitter, through the mirror system, and onto the opaque material. The light is then reflected off the sample, back through the mirror system, through the objective, and upward through the ocular. Total magnification with the ocular furnished by the factory is $25\times$. When working with silicate minerals it becomes desirable to use thin-sections; hence the need for a transmitted light optical system. A transmitted light illuminator was attached to the base of the top cover assembly (see Fig. 1). The light passes through the sample, onto the mirror system, through the objective, and upward through the ocular, over which may be mounted a cap nicol analyzer. Cross nicols or plane light may be obtained by simply rotating the cap nicol 90° . The result is polarized, transmitted light which greatly facilitates the identification of most silicate minerals.

Selected areas within a mount may be accurately positioned in the X-ray path by means of a two-axis micrometer drive stage. The micrometers are accurate to 0.0001 in. The sample holder will take a specimen up to 2 inches in diameter. Scanning permits the analysis of any spot on an area up to 1 inch in diameter, and a worm gear allows the sample to be rotated during the operation.

Inasmuch as the basic instrument is a standard Philips X-ray fluorescent spectrograph, it is not necessary to describe its various components. Bulk rock analyses for major elements utilizing the standard X-ray spectrograph have been described by Volborth (1963) and Hooper (1964), as well as others. Operating conditions comparable to those used in standard X-ray spectrographic work were used and are tabulated in Table 1. Two points of clarification might be made, however. First, the typical collimators used in the standard spectrograph are removed when

operating the macroprobe, and one of three adjustable "anti-scatter slits" may be mounted between the sample and crystal in the crystal housing. The slit chosen should yield the optimum peak/background ratio and count rate. Secondly, note that high order lines are used, rather than the first order lines generally used in standard X-ray spectroscopy. The third and fifth order lines reported in Table 1 were experimentally determined to yield maximum count rates for a given standard.

TABLE 1. INSTRUMENT SETTINGS

| Element radiation | Order | 2θ (mica crystal) | | Target excitation- W tube | Path | PHA base- volts | PHA window- volts | Detector voltage | Detector | Anti-scatter slit |
|-------------------|-------|--------------------------|------------|------------------------------|------|--------------------|----------------------|------------------|------------|-------------------|
| | | Peak | Background | | | | | | | |
| K K_{α} | 3 | 68.53 | 67.50 | 50 kv | vac. | 12 | 20 | 1720 | flow prop. | 10 mm. |
| | | | | 45 ma | | | | | | |
| Ca K_{α} | 3 | 60.72 | 59.10 | 50 kv | vac. | 18 | 20 | 1740 | flow prop. | 10 mm. |
| | | | | 45 ma | | | | | | |
| Ti K_{α} | 3 | 48.87 | 47.30 | 50 kv | vac. | 26 | 18 | 1740 | flow prop. | 10 mm. |
| | | | | 45 ma | | | | | | |
| Mn K_{α} | 5 | 63.65 | 64.80 | 50 kv | vac. | 17 | 26 | 940 | scint. | none |
| | | | | 45 ma | | | | | | |
| Fe K_{α} | 5 | 58.13 | 56.60 | 50 kv | air | 4 | 20 | 840 | scint. | none |
| | | | | 35 ma | | | | | | |

The higher order lines yield greater intensities because at larger 2θ angles all the area of the impinging X-ray beam is contained on the crystal, which may not be the case with the larger beam at lower 2θ angles.

INSTRUMENTAL TESTS

In addition to the usual tests performed before any X-ray fluorescent work, which include those involved in obtaining optimum peak/background ratios and count rates, the unique situation of analyzing small surface areas on individual crystals called for special considerations. Four tests were performed: (1) determination of actual irradiated spot size with each of the four apertures (50, 100, 250, 500 μ in diameter); (2) determination of relative count rates for each aperture; (3) determination of optimum thickness of the thin-section to insure an infinitely thick source of secondary X rays; and (4) determination of the effect of crystallographic orientation on count rate.

Apertures of 500, 250, 100, and 50 μ may be rapidly interchanged from their X-ray port position. The diameter of the area actually being irradiated for each aperture, when the aperture to sample distance is at the optimum setting, is nearly double the aperture diameter. The optimum setting is achieved when the center of the irradiated spot is as close as possible to the center of the crosshairs as seen through the ocular. For example, the spot diameter for the 500 μ aperture was found to be 940 μ , whereas the 250 μ aperture gave a spot size of 460 μ . These actual spot diameters were determined by measuring intensity of Fe X radiation along a traverse across a pyrite fragment embedded in bakelite. The procedure is outlined in the instruction manual and is illustrated graphically in Figure 2, a plot of intensity of Fe radiation *vs.* micrometer distance for the 500 and 250 μ apertures. The distance from maximum intensity to minimum intensity yields the spot size diameter.

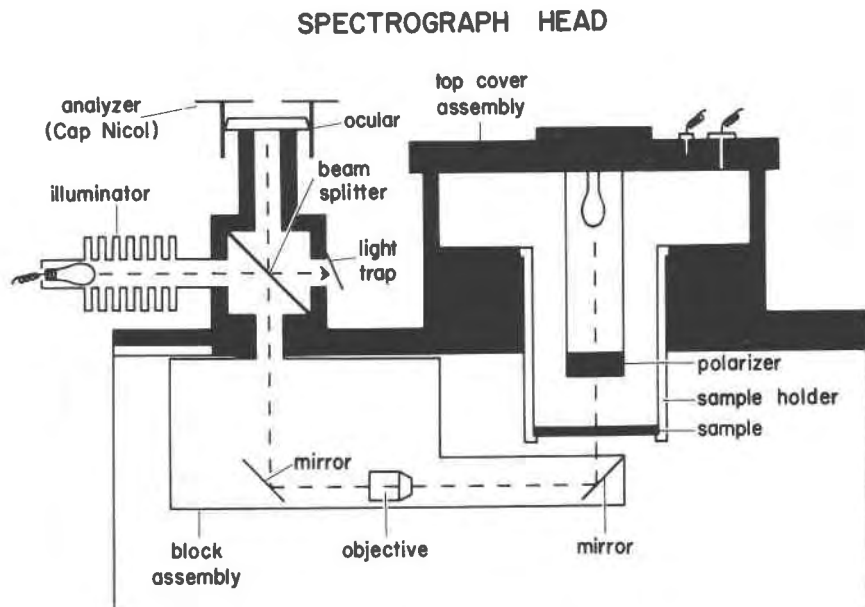


FIG. 1. Schematic diagram of the spectrograph head showing the reflected and transmitted light optics systems.

It is obvious that the larger the aperture the faster is the count rate. These relationships are shown in Table 2, a comparison of count rates for each element and aperture. The data are calculated so that the 500 micron aperture will yield 100 counts per second for each element and the count rates for the other apertures are expressed in relation to it. It is

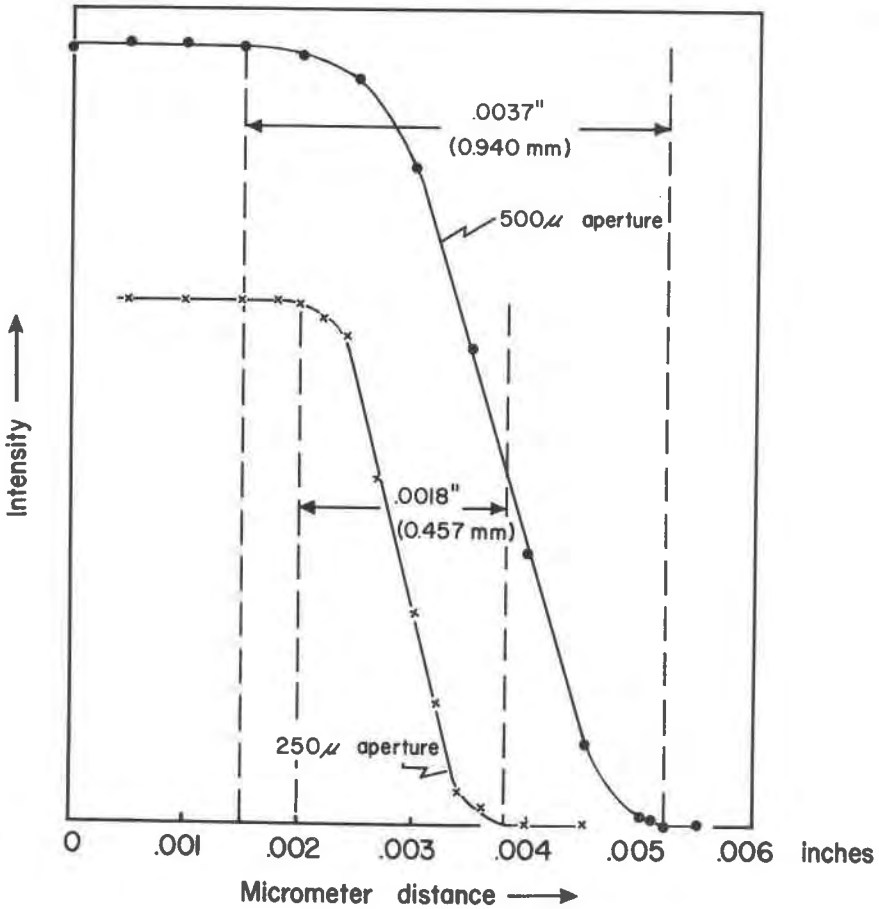


FIG. 2. Plot of intensity of Fe radiation vs. micrometer distance when scanning over a contact between pyrite and bakelite. The distance traversed between the maximum and minimum count rate for each aperture is equal to the diameter of the aperture.

seen from Table 2 that the count rate for the 250 micron aperture is only approximately 30 percent of the 500 micron aperture. With the 100 micron aperture the count rate is approximately 3 percent of the 500 micron aperture, and the count rate is further reduced to only approximately 1 percent with the 50 micron size. These relative count rates are as expected, since the count rate will be about proportional to the area of irradiated spot. Because of the low count rates for the 50 and 100 micron apertures, only Fe yielded sufficiently high count rates in ferromagnesian silicates to be analyzed using these smaller apertures. Thus, with the ex-

ception of Fe, the practical lower limit for the diameter of the irradiated spot is 460 microns (the 250 micron aperture), about equal to the value quoted in Adler and Axelrod (1957)

In standard X-ray spectroscopy, the pellet is usually so thick that the secondary X rays can be considered to be emitted from an infinitely thick source. This is not the case with a standard petrographic thin-section, which is carefully cut to a 30-micron thickness. Koh and Caugherty (1952) measured the critical thickness of Ni, Fe, and Cr plated on Al and found it to be about 30 μ . If elements such as Ni, Fe, and Cr are incorporated in a much lighter matrix, such as a silicate, one would expect the depth of penetration of their characteristic X radiation to be even greater

TABLE 2. RELATIVE COUNT RATES FOR EACH APERTURE

| Aperature size Element | 500 μ | 250 μ | 100 μ | 50 μ |
|---------------------------|-----------|-----------|-----------|----------|
| Fe | 100 | 30.6 | 3.1 | 0.8 |
| Mn | 100 | 35.9 | 4.0 | 0.9 |
| Ti | 100 | 28.1 | 2.4 | 0.6 |
| Ca | 100 | 29.9 | 2.8 | 0.6 |
| K | 100 | 28.5 | 2.5 | 0.6 |

than 30 μ . Figure 3, a plot of intensity for Ca and Fe *vs.* thickness of an augite section, indicates that the thin-section must be at least 70 μ thick. It should be even thicker for the heavier elements. The test was performed by mounting an augite fragment in plastic between two quartz crystals. A slice was taken through the embedded crystals parallel to the quartz *c*-axis. The section was purposely made slightly wedge-shaped, which allowed the true thickness of the augite anywhere along its length to be ascertained by observing the birefringence of the quartz crystals. The intensity of X radiation was recorded as a function of thickness, yielding a critical thickness of about 70 μ for Fe. One would expect the critical thickness to be less for Ca, as it is a lighter element whose X rays have a lesser depth of penetration. This seems to be substantiated by the fact that the intensity of the Ca radiation reaches a plateau at a slightly smaller thickness than does Fe intensity (Fig. 3).

The final test was to determine if differences in crystallographic orientation had any effect on X-ray intensity. The data are shown in Table 3. Slices of various orientations through hornblende and augite indicate that X-ray intensity values remain within the instrumental counting error. Biotite cut perpendicular to cleavage seems to yield lower values

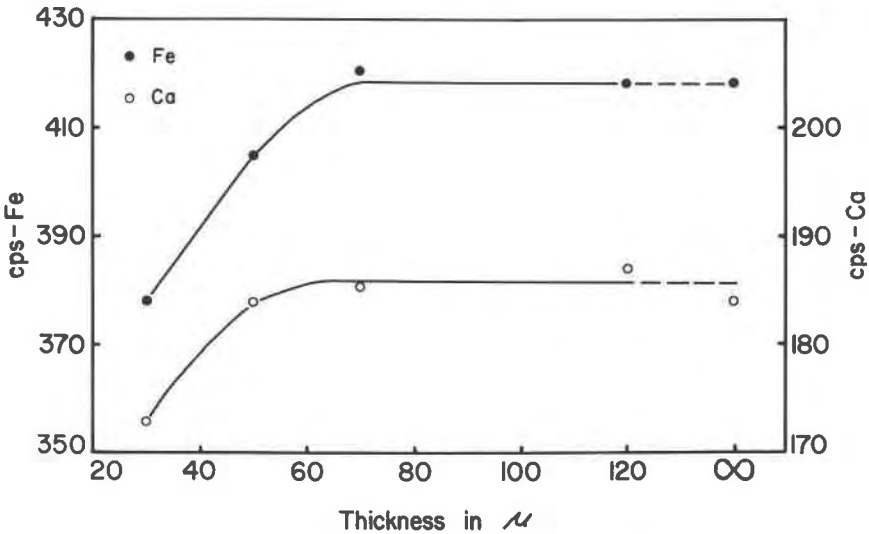


FIG. 3. Plot of intensity of Fe and Ca radiation vs. thickness of an augite thin-section
Note that both intensities reach a plateau at about 70 microns.

than biotite cut parallel to cleavage. Biotite specimens used in this test were small books of biotite which exhibited parting parallel to cleavage. This parting would yield a lower density of atoms perpendicular to cleavage than parallel to cleavage, resulting in lower intensities.

Another consideration was the surface of the thin-section. After testing several methods of grinding and polishing, the method that yielded the best results was to grind the surface with -600 mesh carborundum abrasive in the last step. This yielded reproducible results across one specimen and from one specimen to another of the same composition. Further grinding or polishing did not increase the count rates.

TABLE 3. INTENSITY OF Fe RADIATION AS A FUNCTION OF CRYSTALLOGRAPHIC ORIENTATION

| Mineral | Orientation | Element | cps |
|------------|-------------------------------|---------|------|
| Hornblende | cut \parallel <i>c</i> axis | Fe | 560 |
| | cut \perp <i>c</i> axis | Fe | 570 |
| Augite | cut \parallel —parting | Fe | 1070 |
| | cut \perp —parting random | Fe | 1070 |
| Biotite | cut \perp —cleavage | Fe | 1090 |
| | cut \parallel —cleavage | Fe | 760 |
| | | Fe | 820 |

CALIBRATION

Suitable homogeneous standards of known composition to be used for calibration of the macroprobe were not available and had to be made. Although the ideal situation would be to use ferromagnesian minerals carefully analyzed by other methods as standards, such a procedure is not

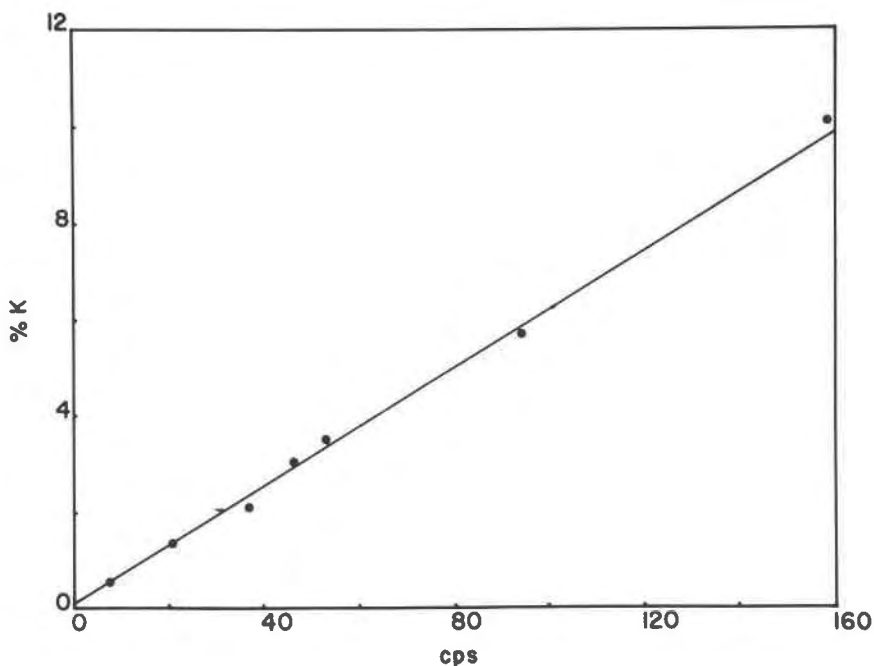


FIG. 4. Potassium calibration curve for 500 μ aperture.

always practical. Minerals that cover a sufficiently wide range of compositions may not be available and those available may not be homogeneous. Thus it was decided to make glass standards by melting rocks and minerals of various compositions.

The glasses were prepared and subsequently analyzed in triplicate by atomic absorption spectrophotometry (for total Fe, Mn, Ca, and K) and colorimetry (for Ti). Accuracy was determined by analyzing the rock standards W-1 and Canadian syenite along with the glasses. Values for the rock standards were within 2 percent of the accepted values (Ingamells and Suhr, 1963). A chip of each glass was then mounted in bakelite and ground off to a flat, smooth surface, the glasses mounted in bakelite were irradiated in the macroprobe unit using the 500 micron aperture,

and the resulting intensities in c.p.s. were plotted *vs.* concentration as determined by atomic absorption or colorimetry.

The resultant calibration curves are shown in Figures 4-8. All the lines of best fit are linear and, with the exception of Mn, pass fairly close to the origin. The line of best fit for Mn (Fig. 7) intercepts the intensity

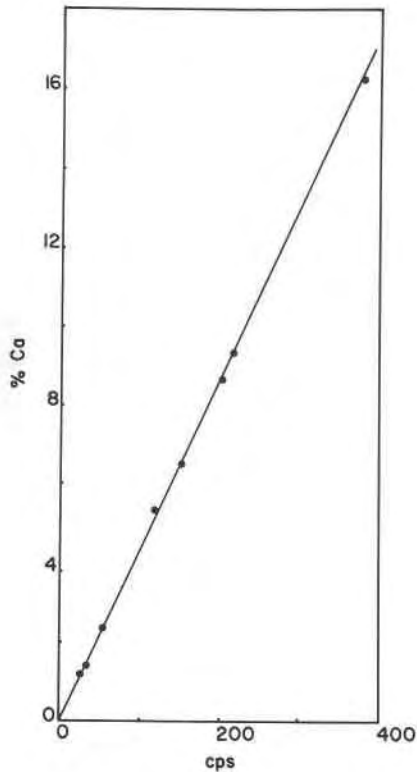


FIG. 5. Calcium calibration curve for 500 μ aperture.

axis at about 5 cps, which suggests Mn impurities in the target of the tungsten X-ray tube.

One might expect the Fe curve to flatten out with increasing Fe due to self-absorption, since Fe is a comparatively heavy element in a light matrix and the range of the calibration curve extends up to 30 percent Fe. This does not seem to be the case, for the most concentrated Fe standard falls close to the linear curve (see Fig. 8). However, several minerals analyzed by atomic absorption and the macroprobe yield systematically low values for Fe on the probe (see Table 4), which suggests that the

curve should be flattened. This implies that the fact the most concentrated standard falls so close to the linear curve is fortuitous. As discussed later, these high atomic absorption values might be explained by contamination.

Although in general the data fall along the lines of best fit very closely, there are deviations, and these deviations may be explained by different

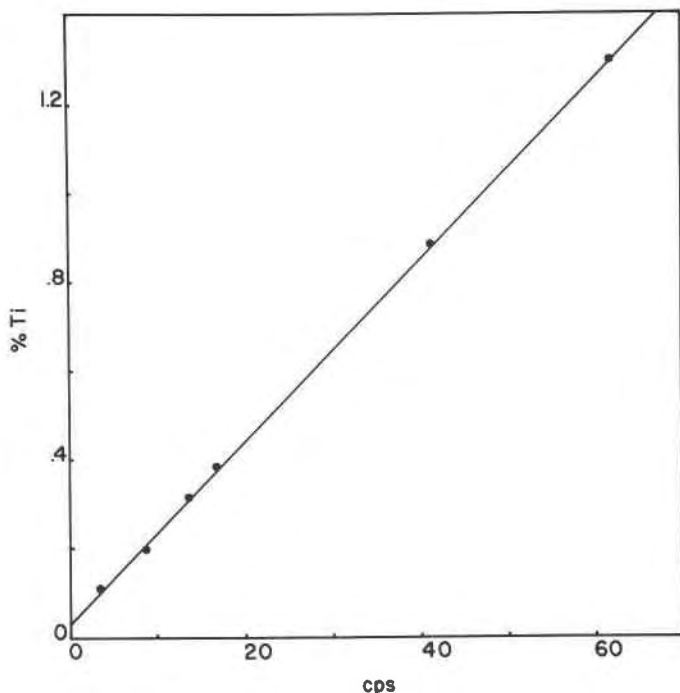


FIG. 6. Titanium calibration curve for 500μ aperture.

matrices and different concentrations of interfering elements. For example, it has been recognized that if the absorption edge of an element is just to the long wavelength side of a characteristic peak of the other element, a mutual interference will occur. The intensity of the first element will be enhanced and the intensity of the second element will be depressed. Thus an increase in Ni content ($K\alpha$ peak for Ni is 1.659 \AA) of a sample will cause an apparent increase in Fe content (K absorption edge for Fe is 1.743 \AA), whereas an increase in Fe content will cause an apparent decrease in Ni. These relationships have been discussed by Brissey *et al.* (1954).

In the case of K and Ca, the potassium K absorption edge at 3.436 \AA is

to the long wavelength side of the calcium $K\alpha$ peak at 3.359 \AA , so an increase in Ca content of the rock should cause an apparent increase in K content, and *vice versa*. In Figure 4, a plot of percent K *vs.* intensity measured in c.p.s., the two values that deviate from the curve the most are at about 10 percent and 2 percent K. The 10 percent K standard, which plots on the low intensity side of the line, is a K-feldspar with very low Ca

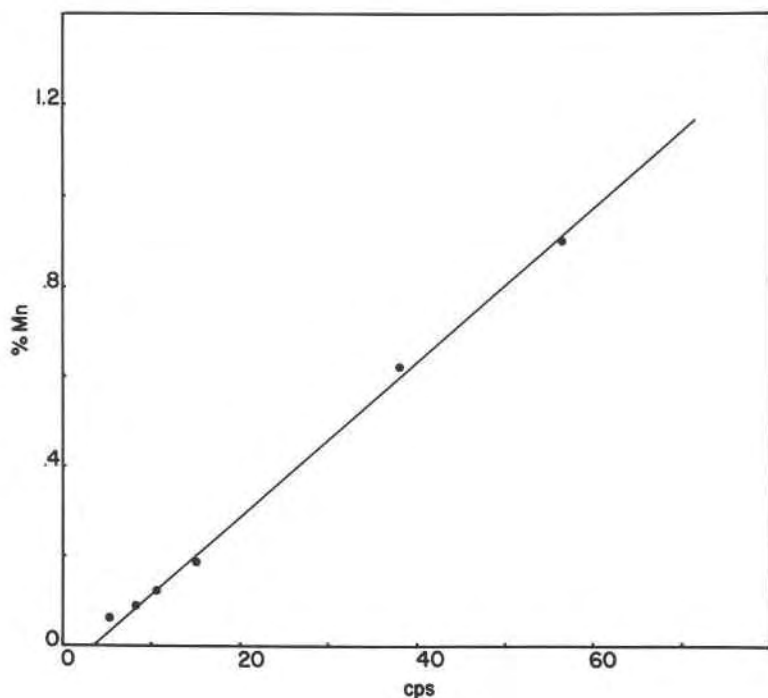


FIG. 7. Manganese calibration curve for 500μ aperture.

content, less than 1 percent. The percent K standard, which plots high, is a calcareous shale, with greater than 10 percent Ca. Thus the location of these two points with respect to the line of best fit seems to substantiate Ca enhancement on the analysis of K. Deviations from the lines of best fit for the other elements might be explained by similar reasoning.

In order to check the validity of the macroprobe to yield accurate as well as precise results, four hornblendes, four biotites, one clinopyroxene, one garnet, and one epidote were analyzed by atomic absorption spectrophotometry and by colorimetry. They were then analyzed with the macroprobe. The comparative values are given in Table 4. Agreement between the two methods for Ca, K, and Ti is invariably within 10 percent

and commonly within 5 percent. Agreement for all elements in the biotites, hornblendes, and clinopyroxene was within 10 percent. Very poor agreement was obtained, however, for Fe in garnet and Mn in garnet and epidote. In the case of Mn and Fe in garnet, the macroprobe values are much too high. The garnet is an almandine garnet, thus there should be no element present to enhance the intensity of the Mn or Fe radiation.

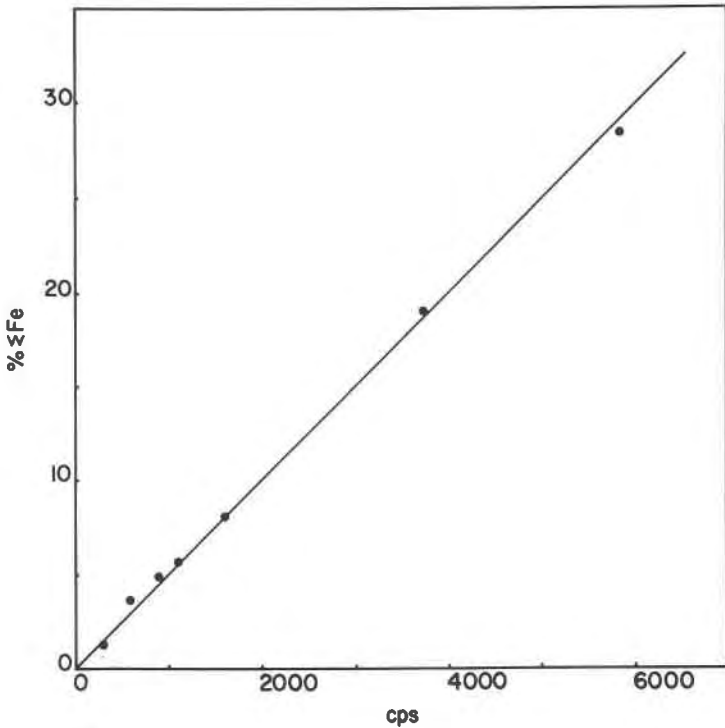


FIG. 8. Iron calibration curve for 500 μ aperture.

Moreover, there is little difference in the mass absorption coefficients for any of the analyzed minerals. For example, the approximate mass absorption coefficients of the analyzed biotites for radiation of 0.71 Å ranges from 10.2 in no. 4 to 7.2 in no. 1, whereas a similar value for the garnet is about 9.3. No inclusions were noted in thin-section. Thus the only apparent explanation is inhomogeneity in the sample with respect to Fe and Mn. The same explanation is offered for the low Mn value from the macroprobe in epidote.

The low macroprobe values for Fe at higher concentrations in the hornblendes and clinopyroxene mentioned earlier may be explained by

TABLE 4. AGREEMENT BETWEEN X-RAY PROBE AND OTHER METHODS

| Sample | Fe | | Ca | | K | | Ti | | Mn | | | | |
|---------------|-------|-------|--------|-------|-------|--------|------|-------|--------|-------|-------|--------|-------|
| | AA | Probe | % dev. | AA | Probe | % dev. | AA | Probe | % dev. | AA | Probe | % dev. | |
| Biotite | 1 | 8.17 | +0.6 | b.d. | 7.69 | 7.42 | -3.5 | 0.67 | 0.73 | +9.0 | 0.15 | 0.14 | |
| | 2 | 14.06 | -7.9 | b.d. | 7.46 | 7.28 | -2.4 | 1.32 | 1.29 | -2.3 | 0.78 | 0.73 | |
| | 3 | 11.43 | -1.6 | b.d. | 7.38 | 7.46 | +1.1 | 1.35 | 1.38 | +2.2 | 0.23 | 0.25 | |
| | 4 | 16.90 | +3.6 | b.d. | 7.50 | 7.52 | +0.3 | 0.72 | 0.75 | +4.2 | 0.76 | 0.80 | |
| Hornblende | 1 | 5.87 | +4.8 | 7.72 | 7.50 | -2.8 | b.d. | 0.57 | 0.57 | 0.0 | b.d. | b.d. | |
| | 2 | 17.14 | -10.1 | 7.51 | 7.20 | -4.1 | 1.61 | 0.28 | 0.27 | -3.6 | 1.09 | 1.05 | |
| | 3 | 17.07 | -9.5 | 7.24 | 7.46 | +3.0 | 1.26 | 0.49 | 0.45 | -8.2 | 0.77 | 0.80 | |
| | 4 | 16.90 | -4.3 | 7.60 | 7.32 | -3.7 | 1.50 | 0.46 | 0.47 | +2.2 | 0.94 | 0.91 | |
| Clinopyroxene | 14.00 | 12.75 | -8.9 | 16.29 | 16.54 | +1.5 | b.d. | b.d. | b.d. | 0.78 | 0.72 | -7.7 | |
| Epidote | 10.70 | 9.80 | -8.4 | 16.88 | 17.64 | +4.5 | b.d. | 0.09 | 0.10 | +11.0 | 0.24 | 0.15 | -37.5 |
| Garnet | 16.39 | 20.90 | +27.5 | 2.83 | 2.98 | +5.3 | b.d. | b.d. | b.d. | 0.38 | 0.52 | +36.8 | |

NOTE: AA denotes atomic adsorption spectrophotometry; color. represents colorimetry; b.d. represents below detection.

minute opaque inclusions observed in thin-section. These inclusions were virtually impossible to separate by heavy liquids or the magnetic separator, so they were digested and analyzed by atomic absorption along with the minerals. They could be avoided, however, when the minerals were analyzed with the probe.

The counting statistics and reproductibility tests are presented in

TABLE 5. COUNTING STATISTICS AND REPRODUCIBILITY

| Element | Counting statistics ¹ | | | | | Reproducibility of standard sample ² | |
|---------|----------------------------------|-----------------------|------------|-----------------------|------------|---|-----|
| | No. counts on peak | Min. peak: background | $\sigma\%$ | Max. peak: background | $\sigma\%$ | V | n |
| K | 20,000 | 2 | 1.73 | 15 | 0.78 | 2.98 | 34 |
| Ca | 20,000 | 5 | 0.97 | 45 | 0.73 | 1.70 | 23 |
| Ti | 20,000 | 2 | 1.73 | 10 | 0.82 | 1.35 | 15 |
| Mn | 10,000 | 2 | 2.44 | 23 | 1.07 | 1.81 | 35 |
| Fe | 80,000 | 9 | 0.42 | 97 | 0.36 | 2.54 | 20 |

¹ Counting error, $\sigma\%$, is defined here as coefficient of variation for the peak taking into account the intensity of the background. $\sigma\%$ is defined as:

$$\sigma\% = 100 (N_P + N_B)^{1/2} / (N_P - N_B)$$

Where N_P is total counts measured at the peak and N_B is number of counts measured on the background.

² Reproducibility is measured as coefficient of variation, V , with n determinations on the same standard sample. V is defined as:

$$V = \frac{100 S}{\bar{x}}$$

Where S is the standard deviation and \bar{x} is the arithmetic mean of the values.

Table 5. Note that the coefficient of variation for the reproducibility of a standard sample (V) is usually equal to or greater than the counting error ($\sigma\%$). It should be mentioned here that some references (see Birks, 1959, p. 52) refer to V in Table 5 as the observed counting error ($\sigma_{\text{obs.}}$), whereas σ percent is called the expected counting error ($\sigma_{\text{exp.}}$). The standard sample was repeatedly counted between other analyses over a period of several days; therefore, its counting precision is subject to instrumental drifts and different instrumental conditions. It is interesting to note that the instrument was so stable for the analyses of Ti and Mn that the coefficient of variation is within the range of the counting error.

CONCLUSIONS

The macroprobe appears to be a satisfactory instrument for the rapid, nondestructive determination of selected elements in minerals which avoids the necessity of performing mineral separations. Needless to say, it has its limitations. One obvious limitation is the slow counting rates when using the small apertures, as shown in Table 6. It can be seen that to achieve 10,000 counts above background for 1 percent K using the 50 μ aperture would require over 24 hours. Owing to extremely slow counting rates, the analysis of Mg and Al in major rock forming silicates with the mica crystal is probably not feasible, even with the largest aperture.

TABLE 6. APPROXIMATE TIME IN MINUTES NECESSARY TO ACCUMULATE 10,000 COUNTS ABOVE BACKGROUND IN ORDER TO DETERMINE 1% OF THE ELEMENT PRESENT

| Element/ Aperture | 500 | 250 | 100 | 50 |
|----------------------|-----|-----|-----|------|
| 1% K | 10 | 36 | 420 | 1700 |
| 1% Ca | 7.2 | 24 | 260 | 1190 |
| 1% Ti | 3.6 | 13 | 150 | 590 |
| 1% Mn | 2.7 | 7.6 | 69 | 300 |
| 1% Fe | 0.8 | 2.7 | 27 | 104 |

However, this situation improves with the heavier elements, and it is very probable that the quantitative analyses of such elements as Rb, Sr, and Ba in feldspars (whose concentrations usually amount to several hundred parts per million) is possible.

Another limitation is, of course, the large spot size compared with the microprobe. Studies on individual minerals generally must be limited to plutonic rocks. In some instances, however, this large spot size may be an advantage. For example, as far as applying the compositions of perthites to the petrogenesis of their plutonic host rocks, it is more important to determine the composition of the entire feldspar before exsolution, rather than determine the composition of the exsolved material. In other words, in some instances the microprobe may give too fine resolution and may be too sophisticated an instrument for the problem at hand. An additional advantage of the macroprobe is the ease and rapidity with which a selected area may be visually located and positioned in the X-ray beam. The comparative simplicity of operation and low initial cost make the macroprobe a useful tool for certain studies in mineralogy, petrology, and geochemistry.

ACKNOWLEDGMENTS

The writers wish to express their thanks to Dr. W. C. Hackler for his aid in making the glasses used for standards. The X-ray macroprobe, power supply, and circuit panel were purchased through a grant to Paul C. Ragland from the North Carolina Board of Science and Technology.

REFERENCES

- ADLER, I. AND J. M. AXELROD (1957) Reflecting curved-crystal X-ray spectrograph—a device for the analysis of small mineral samples. *Econ. Geol.* **52**, 694–701.
- BIRKS, L. S. (1959) *X-Ray Spectrochemical Analysis*, Interscience, New York.
- BRISSEY, R. M., H. A. LIEBHAFSKY AND H. G. PFEIFFER (1954) Examination of metallic materials by X-ray emission spectrography. *ASTM Spec. Tech. Pub.* **157**, 43–56.
- HOOPER, P. R. (1964) Rapid analysis of rocks by X-ray fluorescence. *Anal. Chem.* **36**, 1271–1276.
- INGAMELLS, C. O. AND N. H. SUHR (1963) Chemical and spectrochemical analysis of standard silicate samples. *Geochim Cosmochim. Acta* **27**, 897–911.
- KOH, P. K. AND B. CAUGHERTY (1952) Metallurgical applications of X-ray fluorescent analysis. *J. Appl. Phys.* **23**, 427–433.
- OGILVIE, R. E. (1962) *Introduction to Electron Beam Technology*, John Wiley, New York.
- (1964) X-ray optics in electron microanalysis. *ASTM Spec. Tech. Pub.* **349**, 17–23.
- VOLBORTH, A. (1963) Total instrumental analysis of rocks. *Nevada Bur. Mines Rep.* **6**.

Manuscript received, June 6, 1966; accepted for publication, September 3, 1966.